



# Analytic solutions and universal properties of sugar loading models in Münch phloem flow

Kaare H. Jensen<sup>a,1</sup>, Kirstine Berg-Sørensen<sup>a</sup>, Søren M.M. Friis<sup>a</sup>, Tomas Bohr<sup>b,\*</sup>

<sup>a</sup> Department of Physics, Technical University of Denmark, DTU Physics Building 309, DK-2800 Kongens Lyngby, Denmark

<sup>b</sup> Center for Fluid Dynamics, Department of Physics, Technical University of Denmark, DTU Physics Building 309, DK-2800 Kongens Lyngby, Denmark

## ARTICLE INFO

### Article history:

Received 3 November 2011

Received in revised form

7 March 2012

Accepted 13 March 2012

Available online 30 March 2012

### Keywords:

Sugar translocation in plants

Phloem loading

Analytic solutions of Münch flow

Osmosis

Biological fluid dynamics

## ABSTRACT

The transport of sugars in the phloem vascular system of plants is believed to be driven by osmotic pressure differences according to the Münch hypothesis. Thus, the translocation process is viewed as a passive reaction to the active sugar loading in the leaves and sugar unloading in roots and other places of growth or storage. The modelling of the loading and unloading mechanism is thus a key ingredient in the mathematical description of such flows, but the influence of particular choices of loading functions on the translocation characteristics is not well understood. Most of the work has relied on numerical solutions, which makes it difficult to draw general conclusions. Here, we present analytic solutions to the Münch–Horwitz flow equations when the loading and unloading rates are assumed to be linear functions of the concentration, thus allowing them to depend on the local osmotic pressure. We are able to solve the equations analytically for very small and very large *Münch numbers* (e.g., very small and very large viscosity) for the flow velocity and sugar concentration as a function of the geometric and material parameters of the system. We further show, somewhat surprisingly, that the constant loading case can be solved along the same lines and we speculate on possible universal properties of different loading and unloading functions applied in the literature.

© 2012 Elsevier Ltd. All rights reserved.

## 1. Introduction

Sugar transport in the phloem vascular system of plants is believed to be driven by an osmotically generated pressure difference, as first proposed by Münch in the 1920s (Münch, 1930). According to Münch, sugar produced in the leaves generates an osmotic pressure which drives a flow of water and sugar from source to sink, in accordance with the basic needs of the plants.

The quantitative understanding of this flow mechanism has improved greatly in the last decade through both experimental and theoretical works (Knoblauch and Peters, 2010). Theoretical models of osmotically driven phloem flow are typically based on a number of simplifying assumptions regarding the physiology of the plant: (i) Any gradients in the apoplastic water potential are neglected, (ii) The osmotic pressure is a linear function of the concentration, (iii) The viscosity of the sugar-solution does not depend on the sugar concentration, (iv) The velocity field, the concentration and the pressure are essentially one-dimensional and can be modelled as a function of a single parameter, (v) The presence of sieve plates does not affect the flow aside from a change in the effective viscosity, (vi)

The phloem can be modelled as a collection of individual phloem tubes, with no interaction between parallel tubes and with each of these tubes spanning the entire length of the plant.

An important component in theoretical models of phloem flow is the choice of sugar loading and unloading functions, i.e. the quantitative description of the process of adding sugar to and removing sugar from the phloem vascular system in source and sink tissues. The biochemical processes that control these are not yet fully understood (Turgeon, 1989) but several different models have been used, see e.g. (Christy and Ferrier, 1973; Goeschl and Magnuson, 1986; Minchin et al., 1993; Thompson and Holbrook, 2003a–c, 2004; Thompson, 2005, 2006; Lacoite and Minchin, 2008; Jensen et al., 2011). In most cases the sugar loading rate is assumed to be a function of the local sugar concentration (see e.g. Lacoite and Minchin, 2008), but implicit formulations where the loading function is not specified directly but assumed to lead to certain concentration patterns have also been applied successfully (Jensen et al., 2011). Although some attempts have been made to quantify the effect of the particular choice of loading function on the flow (Goeschl and Magnuson, 1986), it is generally not well understood since most studies have been numerical and thus cover only a small part of the parameter space. Many striking similarities have, however, been observed in the literature among flow solutions with different loading functions (Tyree et al., 1974; Goeschl and Magnuson, 1986; Thompson and Holbrook, 2003b).

\* Corresponding author. Tel.: +45 4525 3310; fax: +45 4593 1669.

E-mail address: [tbohr@fysik.dtu.dk](mailto:tbohr@fysik.dtu.dk) (T. Bohr).

<sup>1</sup> Present address: Department of Organismic and Evolutionary Biology, Harvard University, Cambridge, MA 02138, USA.

In this paper, we derive analytic solutions to steady state Münch phloem flow problems where the loading function is a linear function of the concentration. We use the target concentration formulation (Lacointe and Minchin, 2008), chosen for its availability of a physical interpretation and optional ability to model the transition from source to sink. The solutions fully characterise the axial flow velocity  $u$  and sugar concentration  $c$  as a function of the axial position  $x$  and the geometric and material parameters of the problem. We also discuss the applicability of our solution to more general (Lacointe and Minchin, 2008) concentration dependent loading and unloading functions.

We further show that in some cases, it is possible to transform the concentration dependent loading functions into a constant loading function. This may explain the similarities among flow solutions with different loading functions observed in the literature.

## 2. Mathematical models of loading and unloading in Münch flow

Following Thompson and Holbrook (2003c), we think of the plant as consisting of a single cylindrical phloem tube split into three zones: A loading zone (source, zone 1,  $0 < x < x_1$ ) of length  $l_1$ , a translocation zone (zone 2,  $x_1 < x < x_2$ ) of length  $l_2 = 1$ , and an unloading zone (sink, zone 3,  $x_2 < x < x_3$ ) of length  $l_3$ , see Fig. 1. The steady-state non-dimensional equations of motion for the one-dimensional velocity  $u_i$  (index  $i$  refers to zone number) and sugar concentration  $c_i$  of phloem sap in each of these zones are the Münch–Horwitz equations (Horwitz, 1958; Thompson and Holbrook, 2003c)

$$\partial_x^2 u_i = \partial_x c_i + M\ddot{u} u_i, \tag{1}$$

$$\partial_x(c_i u_i) = \Upsilon_i. \tag{2}$$

The main points in the derivation of Eqs. (1) and (2) are given in Appendix A whereas Table E2 of Appendix E provides a list of parameters. In Eq. (2), the loading function  $\Upsilon_i$  specifies the rate at which sugar is added to or removed from the phloem in the source and sink regions. It is discussed further in Section 2.2, but note that in the translocation zone ( $x_1 < x < x_2$ ) there is no loading and consequently  $\Upsilon_2 = 0$ .

In Eq. (1), the Münch number  $M\ddot{u}$  is the ratio of axial to membrane flow resistance. For a phloem sieve tube of radius  $r$  in a plant of length  $L$ , it is given by  $M\ddot{u} = 16L_p\eta L^2/r^3$ , where  $L_p$  is the permeability of the membrane and  $\eta$  is the viscosity of the phloem sap. Typical values of  $M\ddot{u}$  are in the range of  $1-10^3$  (Jensen et al., 2011). As we will demonstrate in later sections, Eqs. (1)–(2) have analytical solutions in the limits of  $M\ddot{u} \ll 1$  and  $M\ddot{u} \gg 1$ . The limit  $M\ddot{u} \ll 1$  is interesting for several reasons. First of all,  $M\ddot{u} \ll 1$  corresponds to the limit where osmosis dominates over friction and thus it reflects a situation of purely osmotically driven flow. Second, all model system experiments in the literature to date (Münch, 1930; Eschrich et al., 1972; Jensen et al., 2009a, 2009b) have  $M\ddot{u} \ll 1$  mainly because of difficulties in producing liquid channels with dimensions small enough to mimic the biological systems. In addition, as we shall see below, often the numerical solutions corresponding to  $M\ddot{u} \sim 1$  are very similar to the analytical solutions in the limit  $M\ddot{u} \ll 1$ . At the other end, the limit  $M\ddot{u} \gg 1$  is interesting as solutions in this limit obviously may be applied to natural systems with small diameters and long stems.

The boundary conditions imposed on the flow equations are vanishing velocities at the end points

$$u_1(0) = 0, \tag{3}$$

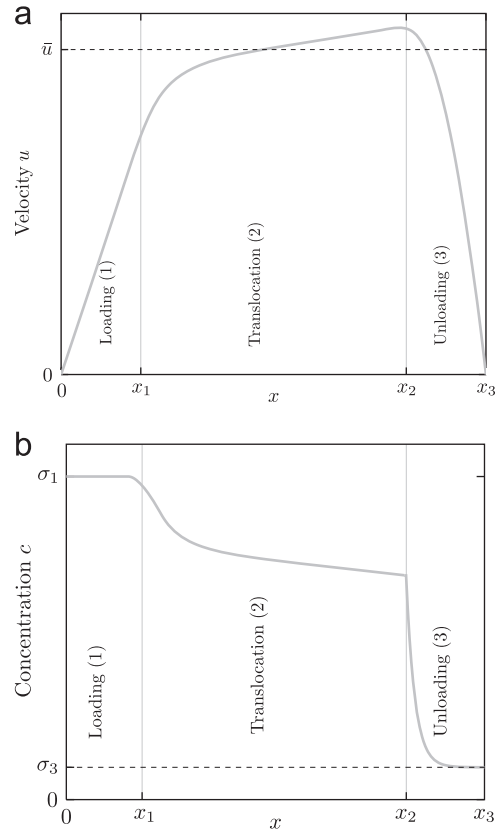


**Fig. 1.** Sketch of characteristic behaviour of the velocity  $u$  and concentration  $c$  derived from numerical solutions of Münch models with a loading, translocation and unloading zone, similar to solutions found in Tyree et al. (1974), Goeschl and Magnuson (1986), Thompson and Holbrook (2003b), Pickard and Abraham-Shrauner (2009). (a) Velocity  $u$  (thick gray line) plotted as a function of axial position  $x$ . The characteristic translocation velocity in the translocation zone  $\bar{u}$  is indicated by the dashed line. (b) Concentration  $c$  (thick gray line) plotted as a function of axial position  $x$ . The concentration at end of the unloading zone  $\sigma_3$  is indicated by the dashed line. See further details in Section 2.1.

$$u_3(x_3) = 0, \tag{4}$$

as well as continuity of  $u$  and  $\partial_x u$  at each of the interior points,  $x = x_1$  and  $x = x_2$ .

$$u_1(x_1) = u_2(x_1), \tag{5}$$

$$\partial_x u_1(x_1) = \partial_x u_2(x_1), \tag{6}$$

$$u_2(x_2) = u_3(x_2), \tag{7}$$

$$\partial_x u_2(x_2) = \partial_x u_3(x_2). \tag{8}$$

Note that continuity of  $\partial_x u$  implies continuity of both the concentration  $c$  and hydrostatic pressure  $p$  since  $\partial_x u \propto (c-p)$ , see Eq. (A.4).

### 2.1. Flow characteristics

The Münch–Horwitz Eqs. (1)–(2) have been studied extensively using numerical solution techniques (Christy and Ferrier, 1973; Goeschl and Magnuson, 1986; Magnuson et al., 1986; Minchin et al., 1993; Thompson and Holbrook, 2003a–c, 2004; Thompson, 2005, 2006; Lacointe and Minchin, 2008), but analytical solutions for systems with both loading, translocation and unloading zones have only been found in a few cases (Pickard and Abraham-Shrauner, 2009; Jensen et al., 2011). Analytical solutions for a single zone may more readily be found, as, e.g., in

Phillips and Dungan (1993) where the translocation zone is investigated.

Although no broad overview of the solutions is currently available, the velocity  $u$  and concentration  $c$  computed from solutions of Eqs. (1)–(8) tend to follow a general pattern, largely independent of the choice of loading function  $\gamma$ , as seen by inspection of the numerical solutions in e.g. Tyree et al. (1974), Goeschl and Magnuson (1986), Thompson and Holbrook (2003b), Pickard and Abraham-Shrauner (2009). The flow velocity  $u$  thus follows the pattern sketched in Fig. 1(a). In the loading zone, it rapidly increases due to the osmotic influx across the semipermeable tube wall. As we move along the translocation zone, the velocity continues to increase as more and more water enter the translocation stream, although at a much slower pace than in the loading zone. In the unloading zone, water gradually exits the tube in response to unloading of sugar before the velocity reaches zero at the end of the unloading zone.

We denote the average velocity in the translocation zone  $\bar{u}$

$$\bar{u} = \frac{1}{x_2 - x_1} \int_{x_1}^{x_2} u_2(x) dx. \tag{9}$$

The concentration  $c$  follows the pattern shown in Fig. 1(b). In the loading zone, it is nearly constant at a level, say,  $c = \sigma_1$ . The characteristic concentration  $\sigma_1$  in the source region is often chosen to be unity due to the non-dimensionalisation of the equations of motion (Jensen et al., 2011). In the translocation zone the concentration is lowered as we move along the  $x$ -axis. This happens because the sugar solution is continually diluted by the influx of water across the membrane due to osmosis. In the unloading zone the concentration decays from an initial level, determined by the flow in the translocation zone, to a level  $c = \sigma_3$  typically much smaller than  $\sigma_1$  as sugar is removed from the tube. The functional form of the decay depends on the choice of loading function, but in many cases it is approximately exponential or linear (Tyree et al., 1974; Smith et al., 1980; Thompson and Holbrook, 2003b).

## 2.2. Loading functions

In most cases the sugar loading rate  $\gamma_i$  is assumed to be a function of the local concentration (see e.g. Lacoite and Minchin, 2008), but implicit formulations where the loading function is not specified directly but assumed to lead to certain concentration patterns have also been applied successfully (Jensen et al., 2011). These two different approaches are discussed in detail in the following two subsections.

### 2.2.1. Implicit loading

In implicit loading schemes, the loading function is not specified directly, but assumed to lead to a prescribed concentration pattern in the loading and unloading zones. As experimental determination of loading and unloading rate constants is difficult (Maynard and Lucas, 1982), this method has the advantage that it only requires knowledge of the characteristic concentrations in the source and sink tissues. With this information and simple assumptions regarding the concentration profiles, comparison between theory and experiment is facilitated.

The implicit loading used by Jensen et al. (2011) assumes a constant concentration  $c = \sigma_1$  in the loading zone, and a linear decay to  $c = 0$  in the unloading zone

$$c = \begin{cases} \sigma_1 & \text{for } 0 < x < x_1, \\ \frac{c_2(x_2)}{x_2 - x_3} (x - x_3) & \text{for } x_2 < x < x_3. \end{cases} \tag{10}$$

Here  $c_2(x_2)$  is a concentration determined by the flow solution in the translocation zone. This implicit loading model reproduces

qualitative and quantitative features found in explicit loading models and is analytically solvable in the limits of very large and very small values of the Münch number  $M\ddot{u}$  (Jensen et al., 2011). A serious shortcoming of the loading scheme given in Eq. (10) is, however, that it treats the loading and unloading zone in an asymmetric way. It will thus never be able to describe, say, the transition from sink to source in a consistent way using Eq. (10). To overcome this obstacle, one could assume a constant concentration in both zones

$$c = \begin{cases} \sigma_1 & \text{for } 0 < x < x_1, \\ \sigma_3 & \text{for } x_2 < x < x_3. \end{cases} \tag{11}$$

As shown in Appendix B, however, this choice of concentration profile is incompatible with Eqs. (1)–(8), since the resulting velocity  $u(x)$  has to be monotonic, thus making the trivial solution  $u = 0$  the only possibility.

### 2.2.2. Explicit loading

In the literature, explicit formulations of the loading or unloading function  $\gamma_i(x)$  is often a linear function in the local concentration  $c_i(x)$

$$\gamma_i(x) = a_i + b_i c_i(x), \tag{12}$$

where  $a_i$  and  $b_i$  are constants whose size and sign determine the rate and direction of the loading. See e.g. Lacoite and Minchin (2008), Eq. (9), and references therein for a detailed discussion of the loading modes contained in Eq. (12). Due to the complexity of the coupled equation system it has thus far only been solved numerically, see e.g. Thompson and Holbrook (2003b), Lacoite and Minchin (2008). Higher order and non-linear loading kinetics have also been used in numerical studies, see e.g. Goeschl and Magnuson (1986). We observe that the numerical results with such Michaelis–Menten like loading dynamics also lead to velocity and concentration profiles that look qualitatively like our sketch in Fig. 1. The added complexity of a non-linear loading and/or unloading thus does not appear to give qualitatively new behaviour. In the work presented here, we have limited ourselves to linear loading and unloading functions, for which it is possible to find analytic solutions.

Since the loading function  $\gamma$  given in Eq. (12) is in non-dimensional form, the biologically relevant choice of parameters  $a_i$  and  $b_i$  are not entirely obvious if, say, we want to preserve the properties of the solution that  $c_1(0) \simeq \sigma_1$  and  $c_3(x_3) \simeq \sigma_3 \ll \sigma_1$ . We thus choose to write the loading function  $\gamma_i$  in a slightly modified form of Eq. (12)

$$\gamma_i = \alpha_i (\sigma_i - c_i), \tag{13}$$

where  $\sigma_i$  is known as a target concentration and  $\alpha_i$  is a measure of the loading rate (Lacoite and Minchin, 2008). In a source region, where sugar is added to the tube, we may interpret the target concentration  $\sigma_i$  as the concentration in the source tissue. In a sink region,  $\sigma_i \ll 1$ , and Eq. (13) simply states that sugar is consumed at a rate proportional to its availability, in agreement with Horwitz’s original formulation of unloading (Horwitz, 1958).

We note that there is a one-to-one correspondence between Eqs. (12) and (13) with  $\alpha_i = -b_i$  and  $\alpha_i \sigma_i = a_i$ , except for the constant loading case with  $a_i = \alpha_i \sigma_i \neq 0$  and  $b_i = -\alpha_i = 0$ . This special case is treated in Appendix C.

For later use, we note that Eqs. (2), (12), (13), (3) and (4) imply that the concentration at the end points ( $x = 0, x = x_3$ ) is given by

$$c_1(0) = \frac{a_1}{\partial_x u_1(0) - b_1} = \frac{\alpha_1 \sigma_1}{\partial_x u_1(0) + \alpha_1}, \tag{14}$$

$$c_3(x_3) = \frac{a_3}{\partial_x u_3(x_3) - b_3} = \frac{\alpha_3 \sigma_3}{\partial_x u_3(x_3) + \alpha_3}, \tag{15}$$

where we assume that the parameters have been chosen such that  $c_1(0) \geq 0$  and  $c_3(x_3) \geq 0$ . From Eqs. (14)–(15), we observe that  $c_1(0) \rightarrow \sigma_1$  when  $\alpha_1 \rightarrow \infty$  and that  $c_3(x_3) \rightarrow \sigma_3$  when  $\alpha_3 \rightarrow \infty$ , if in the same limits  $\partial_x u_1(0)/\alpha_1 \rightarrow 0$  and  $\partial_x u_3(x_3)/\alpha_3 \rightarrow 0$ .

### 3. Analytic solutions of the equations of motion

The following analysis of the equations of motion aims to analytically determine solutions to Eqs. (1)–(8) with loading function  $c$  as a function of the axial position  $x$  and their variation with the parameters of the problem  $M\ddot{u}$ ,  $x_1$ ,  $x_2$ ,  $x_3$ ,  $\alpha_1$ ,  $\alpha_2$ ,  $\alpha_3$ ,  $\sigma_1$ ,  $\sigma_2$  and  $\sigma_3$ . A solution for arbitrary values of the Münch number  $M\ddot{u}$  is not currently available, but the equation system can be solved in the limits of very small and very large values of  $M\ddot{u}$ , as shown in Sections 3.1 and 3.2.

#### 3.1. Solution for $M\ddot{u} \ll 1$

In this limit, we neglect the term including  $M\ddot{u}$  and the equations of motion for the flow velocity  $u$  and concentration  $c$  simplify to

$$\partial_x^2 u_i = \partial_x c_i, \tag{16}$$

$$\partial_x(c_i u_i) = \alpha_i(\sigma_i - c_i). \tag{17}$$

The boundary conditions are as stated in Eqs. (3)–(8).

As discussed below, there is mathematical equivalence between loading and unloading zone, and we therefore solve in these zones simultaneously.

##### 3.1.1. Loading and unloading zones, $i=1,3$

We first note the symmetry of the equations. If we are looking for solutions in the unloading zone  $x_2 < x < x_3$  we can use the variable  $\xi = x_3 - x$ . Using also  $\zeta_i(\xi) = c_i(x)$  and  $\eta_i(\xi) = -u_i(x)$  we see that the Eqs. (16)–(17) are unchanged, i.e.

$$\partial_\xi^2 u_i = \partial_\xi \zeta_i, \tag{18}$$

$$\partial_\xi(\eta_i \zeta_i) = \alpha(\sigma_i - \zeta_i). \tag{19}$$

Thus, to look for a solution before the endpoint  $x_3$  of the unloading zone, we should look for a solution to the right of  $\xi = 0$  with negative velocity. This means that both solutions will represent flow *into* the central point. The conceptual difference between a loading zone and an unloading zone is illustrated in Fig. 2.

In order to simplify the notation, we will in the rest of this subsection use  $x$  for both the original coordinate in the loading zone, and the transformed coordinate  $\xi$  in the unloading zone; also we use the symbol  $c(x)$  for both  $c_1(x)$  and  $\zeta_3(\xi)$  and  $u(x)$  for  $u_1(x)$  and  $\eta_3(\xi)$ .

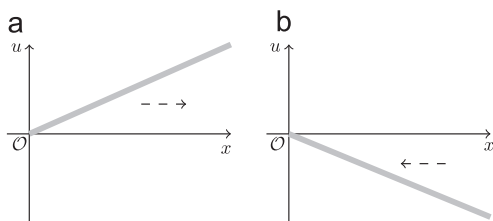


**Fig. 2.** The conceptual difference between source and sink flow into and out of the origin  $\mathcal{O}$ . The flow velocity  $u$  (thick gray line) is plotted as a function of axial position  $x$  for a loading zone (a), and an unloading zone (b) after the coordinate transformation. The dashed arrows indicate the direction of the flow.

Proceeding to solve the flow problem, we begin by integrating Eq. (16)

$$\partial_x u = c(x) - K_1. \tag{20}$$

With the result in Eq. (20), Eq. (17) can be written as

$$\partial_x(cu) = \alpha(\sigma - K_1) - \alpha \partial_x u. \tag{21}$$

Integrating gives

$$uc = \alpha(\sigma - K_1)x - \alpha u + K_2, \tag{22}$$

where  $K_2 = 0$  since we require that  $u(0) = 0$ . Solving Eq. (22) for  $c$  and inserting into Eq. (20) gives

$$\partial_x u = \frac{\alpha_i(\sigma - K_1)x - (\alpha + K_1)u}{u}, \tag{23}$$

where we have now entirely eliminated  $c$ .  $K_1$  is given by

$$K_1 = \frac{\alpha\sigma}{\partial_x u(0) + \alpha} - \partial_x u(0) \tag{24}$$

$$= \frac{\alpha\sigma - \partial_x u(0)^2 - \alpha \partial_x u(0)}{\partial_x u(0) + \alpha}. \tag{25}$$

Eq. (23) is homogeneous of first order in  $u$  and  $x$ . Thus, introducing  $v = u/x$  we get

$$\partial_x(vx) = \frac{\alpha(\sigma - K_1) - (\alpha + K_1)v}{v}, \tag{26}$$

or

$$x \partial_x v = \partial_z v = \frac{\alpha(\sigma - K_1) - (\alpha + K_1)v - v^2}{v}, \tag{27}$$

where  $z = \log x$ . Inverting Eq. (27) gives

$$\partial_v z = -\frac{v}{\mathcal{L}(v)}, \tag{28}$$

where  $\mathcal{L}(v) = v^2 + (\alpha + K_1)v - \alpha(\sigma - K_1) = (v - v_+)(v - v_-)$  and the two roots are given as

$$v_{\pm} = -\frac{1}{2}(\alpha + K_1) \pm \sqrt{(\alpha - K_1)^2 + 4\alpha\sigma} \tag{29}$$

which with Eq. (25) become

$$v_+ = -\frac{\alpha(\partial_x u(0) + \alpha + \sigma)}{\partial_x u(0) + \alpha} = -(c(0) + \alpha), \tag{30}$$

$$v_- = \partial_x u(0). \tag{31}$$

We can now consider the case where the two roots  $v_+$  and  $v_-$  are distinct. Integrating Eq. (28) from  $v_a$  to  $v_b$  (where  $v_-$  and  $v_+$  are not in the interval  $[v_a, v_b]$ ) gives

$$\begin{aligned} z(v_b) - z(v_a) &= \log \frac{x_b}{x_a} \\ &= -\frac{1}{v_+ - v_-} \int_{v_a}^{v_b} \left( \frac{v_+}{v - v_+} - \frac{v_-}{v - v_-} \right) dv \\ &= \log \left[ \left| \frac{v_b - v_+}{v_a - v_+} \right|^{-v} \left| \frac{v_b - v_-}{v_a - v_-} \right|^{\omega} \right], \end{aligned} \tag{32}$$

where

$$v = \frac{v_+}{v_+ - v_-} = \frac{\alpha(\partial_x u(0) + \alpha + \sigma)}{(\partial_x u(0) + \alpha)^2 + \alpha\sigma},$$

$$\omega = \frac{v_-}{v_+ - v_-} = -\frac{\partial_x u(0)(\partial_x u(0) + \alpha)}{(\partial_x u(0) + \alpha)^2 + \alpha\sigma} = v - 1. \tag{33}$$

Exponentiating Eq. (32) we get

$$x_b |v_b - v_+|^v |v_b - v_-|^{-\omega} = x_a |v_a - v_+|^v |v_a - v_-|^{-\omega} \equiv K_3. \tag{34}$$

Reinserting  $v(x) = u(x)/x$ , Eq. (34) may be reformulated as

$$x \left| \frac{u(x)}{x} - v_+ \right|^v \left| \frac{u(x)}{x} - v_- \right|^{-\omega} = x \left| \frac{u(x)}{x} - v_+ \right|^v \left| \frac{u(x)}{x} - v_- \right|^{1-v} = K_3, \tag{35}$$

and gives an implicit solution for  $u(x)$  in terms of the integration constant  $K_1, K_2 = 0$  and  $K_3$ . Eq. (20) subsequently allows for a determination of the concentration  $c(x)$ .

A special case is a solution of Eq. (35) of the form

$$u = A_1 x, \tag{36}$$

which ensures  $u(0) = 0$ . From Eq. (31) we find that  $A_1 = v_-$  and consequently that  $K_3 = 0$ . In order for such a solution to exist, we realise that we must require  $\omega < 0$ , or  $v < 1$ ; cf. Eq. (33). We further observe that the concentration  $c$  is constant and given by

$$c = \frac{\alpha \sigma}{\alpha + A_1}, \tag{37}$$

in agreement with Eqs. (14) and (15).

In the loading zone, we find that the linear solution Eq. (36) is the appropriate one, whereas in the unloading zone the more general case, Eq. (35) applies and no linear solution exists. As we now emphasise differences between loading and unloading zones, we reintroduce the subscripts  $i$  for zone number  $i$  on  $u, c, \alpha$  and  $\sigma$ , and add the subscript  $i$  to integration constants and other quantities that now read  $A_{1,i}, K_{1,i}, K_{2,i}, K_{3,i}, v_{\pm,i}$  and  $v_i, \omega_i$ .

Recall the difference between loading zone and unloading zone, as illustrated in Fig. 2. In the loading zone,  $u_1 \geq 0$  and  $\partial_x u_1(0) > 0$  whereas in the unloading zone,  $u_3 \leq 0$  and  $\partial_x u_3(0) < 0$ . Following the results in Eqs. (30)–(31), this implies that in the loading zone,  $v_{-,1} > 0$ , whereas in the unloading zone,  $v_{-,3} < 0$ . In both cases,  $v_{+,i} < 0$ .

As stated above, the existence of a linear solution requires  $v_i < 1$ . Using the definition of  $v_i$  in Eq. (33), and the expression for the two roots  $v_{\pm,i}$ , Eq. (29), the condition in  $v_i$  may be rewritten into bounds on  $K_{1,i}$ ,

$$-\alpha_i < K_{1,i} < \sigma_i. \tag{38}$$

Eq. (20) defines  $K_{1,i}$ , and Eqs. (14)–(15) specify expressions for  $c_i$  in the loading and unloading zone, to be inserted in the equation for  $K_{1,i}$ .

In the loading zone, since  $\partial_x u_1(0) > 0$ , we see from Eq. (14) that  $c_1(0) < \sigma_1$ . Thus, the upper bound on  $K_{1,1}$  in Eq. (38) is always fulfilled. On the contrary, in the unloading zone, since  $\partial_x u_3(0) < 0$ , Eq. (15) implies that  $c_3(0) > \sigma_3$ . Now, Eq. (20) implies

$$K_{1,3} = c_3(0) - \partial_x u_3(0) = c_3(0) + |\partial_x u_3(0)| > c_3(0) > \sigma_3. \tag{39}$$

Therefore, the condition that  $K_{1,3} < \sigma_3$ , required for a linear solution to exist, is never fulfilled in the unloading zone.

### 3.1.2. Translocation zone, $i=2$

In the translocation zone, there is no loading ( $\alpha_2 = 0$ ) and the equations of motion are

$$\partial_x^2 u_2 = \partial_x c_2, \tag{40}$$

$$\partial_x(c_2 u_2) = 0. \tag{41}$$

Eq. (41) implies sugar flux conservation such that  $c_2(x)u_2(x) = c_2(x_1)u_2(x_1) = c_1(x_1)u_1(x_1)$  for  $x \in [x_1, x_2]$ . We can thus integrate Eq. (40)

$$\partial_x u_2 = \frac{u_1(x_1)c_1(x_1)}{u_2} + A_3. \tag{42}$$

If  $\partial_x u_2 \neq 0$  we can invert this equation

$$\partial_{u_2} x = \frac{u_2}{u_1(x_1)c_1(x_1) + A_3 u_2} \tag{43}$$

such that

$$x(u_2) = \frac{u_2}{A_3} - \frac{u_1(x_1)c_1(x_1)}{A_3^2} \log(A_3 u_2 + u_1(x_1)c_1(x_1)) + A_4^*. \tag{44}$$

Alternatively, we may write

$$x(u_2) = \frac{u_2}{A_3} - \frac{u_1(x_1)c_1(x_1)}{A_3^2} \log \left( \frac{1 + \frac{A_3 u_2}{u_1(x_1)c_1(x_1)}}{1 + \frac{A_3}{c_1(x_1)}} \right) + A_4, \tag{45}$$

a more convenient formulation when evaluating the expression  $x_1 = x(u_2(x_1))$ . If  $\partial_x u_2 \rightarrow 0$ , we find from Eq. (42) that  $u_2$  approaches the value

$$u_2 = - \frac{c_1(x_1)u_1(x_1)}{A_3}. \tag{46}$$

For the concentration  $c_2$ , we have from the flux conservation relation that

$$c_2 = \frac{u_1(x_1)c_1(x_1)}{u_2}. \tag{47}$$

### 3.1.3. Matching of the solution

The solutions for  $M\ddot{u} \ll 1$  in the three zones are of the form

$$u_1 = A_{1,1} x \tag{48}$$

$$x(u_2) = \frac{u_2}{A_3} - \frac{u_1(x_1)c_1(x_1)}{A_3^2} \log \left( \frac{1 + \frac{A_3 u_2}{u_1(x_1)c_1(x_1)}}{1 + \frac{A_3}{c_1(x_1)}} \right) + A_4, \tag{49}$$

$$K_{3,3} = x \left( \frac{u_3}{x} - v_+ \right)^v \left( \frac{u_3}{x} - v_- \right)^{-\omega} \tag{50}$$

To evaluate the constants  $A_{1,i}, A_3, A_4, K_{1,i}$ , and  $K_{2,i}$ , we use the boundary conditions in Eqs. (3)–(8). Note that the constant  $A_{1,i}$  only lives in the loading zone ( $i=1$ ) while  $K_{1,i}$  is only relevant in the unloading zone ( $i=3$ ).  $K_{2,i}$ , on the other hand, must be found in both the loading ( $i=1$ ) and unloading ( $i=3$ ) zones. Continuity of  $u(x)$  at the boundary between translocation and unloading zone, at  $x = x_2$ , links the value of  $K_{3,3} = x_2((u_3(x_2)/x_2) - v_+)^v ((u_3(x_2)/x_2) - v_-)^{-\omega}$  to the other constants. Applying the boundary conditions and using that  $\partial_x u_2(x_2) \simeq 0$  we find six equations in six unknowns, given in Table 1, which allow for a solution of the problem as discussed further in Section 5.

### 3.2. Solution for $M\ddot{u} \gg 1$

The equations of motion are

$$\partial_x^2 u_i = \partial_x c_i + M\ddot{u} u_i, \tag{51}$$

$$\partial_x(c_i u_i) = \alpha_i(\sigma_i - c_i). \tag{52}$$

The boundary conditions are as stated earlier in Eqs. (3)–(8). For large  $M\ddot{u}$  numbers, we observe that the velocity becomes very small, and as we will argue later, decreases with  $M\ddot{u}$  at least as  $1/M\ddot{u}$ . Also, in this limit, the numerical solutions display

**Table 1**  
Evaluation of the constants  $A_1, A_2, A_3, A_4, K_{1,3}$  and  $K_{2,i}$  from the boundary conditions.

Boundary condition	Equation	Ref.
$u_1(0) = 0$	$K_{2,1} = 0$	(3), (22)
$u_3(x_3) = 0$	$K_{2,3} = 0$	(4), (22)
$u_1(x_1) = u_2(x_1)$	$A_4 = x_1 \left( 1 - \frac{A_{1,1}}{A_3} \right)$	(5), (36), (45)
$\partial_x u_1(x_1) = \partial_x u_2(x_1)$	$A_3 = A_{1,1} - \frac{\alpha_1}{\alpha_1 + A_{1,1}} \sigma_1$	(6), (36), (42), (37)
$u_2(x_2) = u_3(x_2)$	$\frac{A_{1,1} x_1 \alpha_1 \sigma_1}{A_3(\alpha_1 + A_{1,1})} = \frac{\alpha_3(\sigma_3 - K_{1,3}) l_3}{\alpha_3 + K_{1,3}}$	(7), (42), (23), (36), (37)
$\partial_x u_2(x_2) = \partial_x u_3(x_2)$	$A_3 = -K_{1,3}$	(8), (42), (20)

boundary layers between the different zones, unlike for small Münch numbers. We therefore consider the loading and the unloading zones separately in our discussion below.

3.2.1. Loading zone,  $i=1$

In order to find an approximate analytical solution in the loading zone, we note that the concentration is almost equal to the constant value  $\sigma_1$ . We thus express  $c_1$  as

$$c_1(x) = \sigma_1 - \epsilon(x), \tag{53}$$

which means that Eq. (52) can be written as

$$\alpha_1(\sigma_1 - c_1) = \alpha_1 \epsilon = \partial_x(c_1 u_1) = \partial_x(u_1(\sigma_1 - \epsilon)) \approx \sigma_1 \partial_x u_1, \tag{54}$$

where we have assumed that  $u_1 \partial_x c_1 \ll c_1 \partial_x u_1$  and  $\epsilon \ll \sigma_1$ . Thus, Eq. (51) becomes

$$\left(1 + \frac{\sigma_1}{\alpha_1}\right) \partial_x^2 u_1 = M\ddot{u} u_1, \tag{55}$$

with the solution

$$u_1(x) = B_1 \sinh(\beta_1 x) + B_2 \cosh(\beta_1 x), \tag{56}$$

where  $B_2 = 0$  since  $u_1(0) = 0$ , and  $\beta_1 = \sqrt{M\ddot{u}/(1 + \sigma_1/\alpha_1)}$ , whereby the approximate solution is

$$u_1(x) = B_1 \sinh(\beta_1 x). \tag{57}$$

Using this approximate solution for the velocity in the loading zone, we may now combine Eqs. (51) and (55) to find the concentration via

$$\partial_x c_1(x) = -\frac{\sigma_1}{\alpha_1 + \sigma_1} B_1 \sinh(\beta_1 x), \tag{58}$$

which, with the boundary condition Eq. (14), is integrated to yield the solution

$$c_1(x) = \frac{M\ddot{u} B_1}{\beta_1} \frac{\sigma_1}{\alpha_1 + \sigma_1} (1 - \cosh(\beta_1 x)) + \frac{\alpha_1 \sigma_1}{\alpha_1 + B_1 \beta_1}. \tag{59}$$

Thus, we see that the front-factor on  $u_1 \partial_x c_1$  is proportional to  $B_1^2 M\ddot{u}$  whereas  $c_1 \partial_x u_1$  contains a term proportional to  $B_1 \beta_1$  in addition to a factor proportional to  $B_1^2 M\ddot{u}$ . With  $B_1 \propto 1/M\ddot{u}$  and  $\beta_1 \propto \sqrt{M\ddot{u}}$ , we can now confirm that our initial assumption of neglecting  $u_1 \partial_x c_1$  in comparison to  $c_1 \partial_x u_1$  is acceptable for  $M\ddot{u} \gg 1$ .

3.2.2. Translocation zone,  $i=2$

In the translocation zone, the equations of motion are

$$\partial_x^2 u_2 = \partial_x c_2 + M\ddot{u} u_2, \tag{60}$$

$$\partial(c_2 u_2) = 0. \tag{61}$$

With a slight modification to our notation, we use the solution for the velocity  $u_2$  found in Jensen et al. (2011),

$$u_2(x) = \frac{u_1(x_1)}{\sqrt{1 - 2M\ddot{u}(u_1(x_1)/c_1(x_1))(x - x_1)}}, \tag{62}$$

which only fulfills the boundary condition Eq. (5), and not Eq. (6). To find  $c_2(x)$ , we note from Eq. (52) that the product  $c_2(x)u_2(x)$  is constant throughout the translocation zone, implying

$$c_2(x) = \frac{c_1(x_1)u_1(x_1)}{u_2(x)}. \tag{63}$$

We note from Eq. (62) that in order for  $u_2(x)$  to stay real and finite even when  $M\ddot{u}$  is large,  $u_1(x_1)/c_1(x_1)$  must decrease with increasing  $M\ddot{u}$  at least as  $1/M\ddot{u}$ . Since  $c_1(x_1)$  is of order  $\sigma_1$ , this implies that  $u_1(x_1)$  decreases with  $M\ddot{u}$  at least as  $1/M\ddot{u}$ .

3.2.3. Unloading zone,  $i=3$

From the numerical solutions shown in Fig. 3, we observe that between the loading zone and the translocation zone, within a narrow interval, the concentration changes abruptly, in a

seemingly exponential fashion—as to readjust its value. However, as we have simplified the equations of motion in the translocation zone to have vanishing transport across the membrane, i.e.,  $\alpha_2 = 0$ , the equations do not point to a specific physical length scale over which this readjustment should take place.

On the contrary, between the translocation zone and the unloading zone, where  $\alpha_3 \neq 0$ , a length scale for a boundary layer, or readjustment length scale, appears in the equations. We find that the numerical solution to the velocity changes only slightly and goes through a maximum a short distance into the unloading zone. Using this insight, we can find an approximate solution to the equations for  $c$  and  $u$  in the unloading zone. As the velocity is almost constant in the boundary layer, we first neglect the term with  $\partial_x u_3$  in Eq. (52), to obtain

$$u_2(x_2) \partial_x c_3 = \alpha(\sigma_3 - c_3). \tag{64}$$

A natural length-scale  $\lambda = u_2(x_2)/\alpha_3$  appears in the equation for  $c$ , and the solution is found as

$$c_3(x) = \sigma_3 + (c_2(x_2) - \sigma_3) \exp(-(x - x_2)/\lambda) \tag{65}$$

when we require that  $c$  is continuous at the end of the translocation zone,  $c_2(x_2) = c_3(x_2)$ .

Inserting this solution, Eq. (65), for  $c_3$  in the remaining equation for the velocity, Eq. (51), results in the complete solution,

$$u_3(x) = B_3 \exp(-(x - x_2)/\lambda) + B_4 \sinh(\sqrt{M\ddot{u}}(x - x_2)) + B_5 \cosh(\sqrt{M\ddot{u}}(x - x_2)), \tag{66}$$

where the constant  $B_3$  is fixed by the differential equation and the result for  $c_3$ , Eq. (65), whereas  $B_4$  and  $B_5$  are fixed by requiring continuity in both  $u$  and  $\partial_x u$  at the position  $x_2$ ; Eqs. (7)–(8). Upon insertion of the result for  $u_2$  and  $c_2$  in the translocation zone, Eqs. (62) and (63), in these requirements for continuity, one finds

$$B_3 = -\frac{(c_2(x_2) - \sigma_3)/\lambda}{1/\lambda^2 - M\ddot{u}}, \tag{67}$$

$$B_4 = \left[ \frac{M\ddot{u} u_2^3(x_2)}{c_1(x_1) u_1(x_1)} + B_3/\lambda \right] / \sqrt{M\ddot{u}}, \tag{68}$$

$$B_5 = u_2(x_2) - B_3. \tag{69}$$

3.2.4. Matching of the solution

In the solutions presented in Sections 3.2.1, 3.2.2, and 3.2.3, we have ensured that the boundary condition given in Eqs. (3) and (5)–(8) is fulfilled. To fulfill the final boundary condition in Eq. (4) we must determine  $B_1$  which enters  $c_1(x_1)$  and  $u_1(x_1)$  in Eq. (68) such that  $u_3$  given in Eq. (66) vanishes at  $x = x_3$ .

It is not possible to give an analytic expression for  $B_1$  and the system of equations that match solutions and boundary conditions just discussed must therefore be solved numerically. In practice, we wrote the equations in Mathematica 8 (Wolfram Research), treating the unknown parameter  $B_1$  as a variable, and found the roots of  $u_3(x_3)$  as a function of  $B_1$ . Note that  $u_3(x_3)$  usually has several roots as a function of  $B_1$ , but only one of these corresponds to real-valued, positive flow solutions.

4. Comparison between analytical and numerical solution

To compare the analytical solutions found in the limiting cases of  $M\ddot{u} \ll 1$  and  $M\ddot{u} \gg 1$  to solutions of the full problem, the equations of motion (1)–(8) and loading function (13) were solved numerically in MATLAB 7.8 (MathWorks, Inc.) using an upwind solver (Press, 2001). After a thorough convergence analysis, numerical solutions similar to

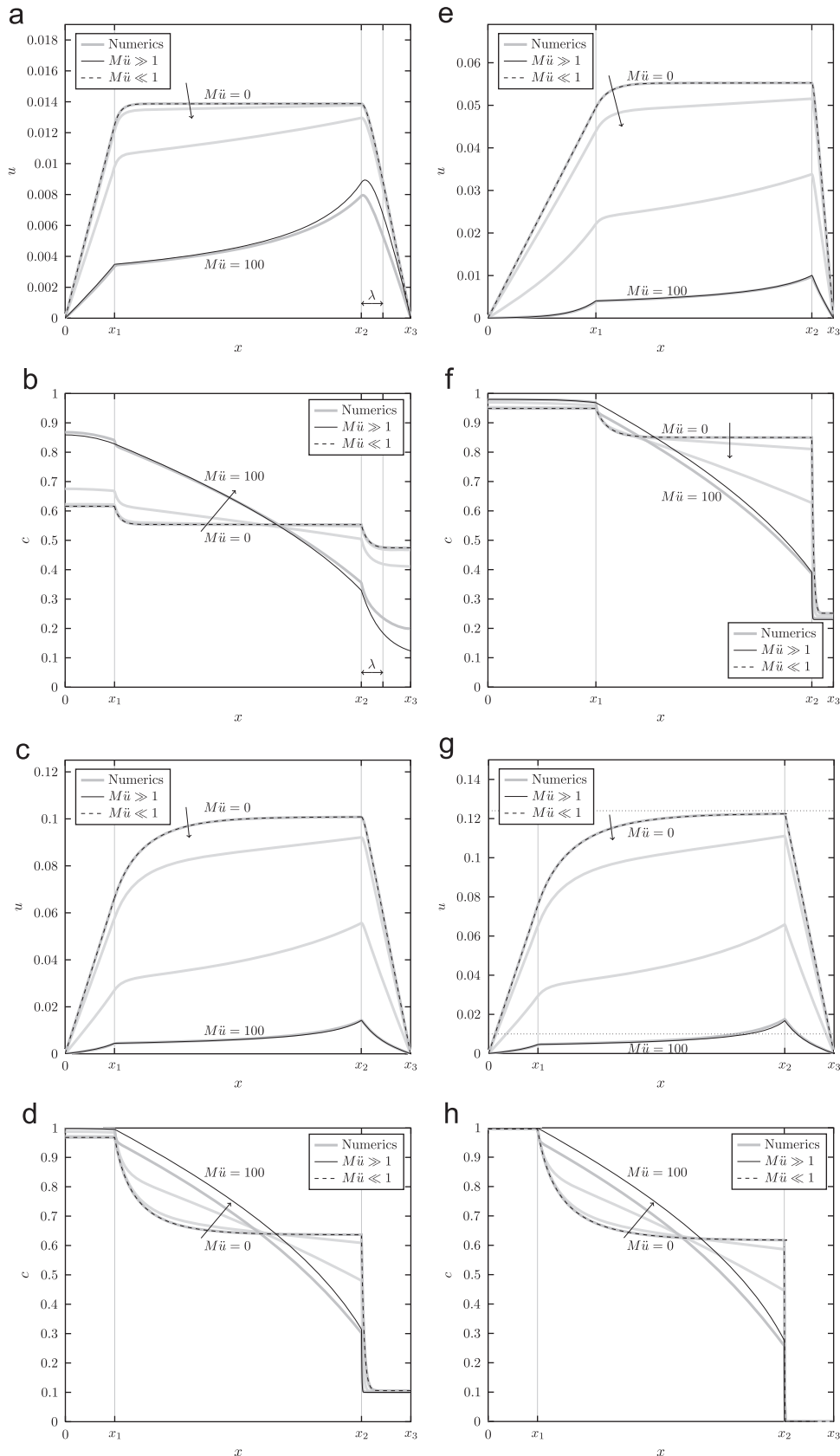


**Fig. 3.** Numerical (thick gray lines) and analytical solutions of Eqs. (1)–(8) and (13) for values of the Münch number  $M\ddot{u} = 0, 1, 10, 100$  increasing along the direction of the solid black arrow ( $\rightarrow$ ). Analytical solutions are given for  $M\ddot{u} = 0$  (thin dashed line) and  $M\ddot{u} = 100$  (thin solid line). (a), (c), (e) and (g): Flow velocity  $u$  plotted as a function of axial position  $x$ . (b), (d), (e) and (h): Concentration  $c$  plotted as a function of axial position  $x$ . The boundary layer thickness  $\lambda$ , cf. Eq. (65), for  $M\ddot{u} = 100$  is indicated by double arrows ( $\leftrightarrow$ ) in (a) and (b). It is not given in (c)–(h) since it is much smaller than  $x_3 - x_2$  in these cases. The dotted horizontal lines in (g) indicate the mean translocation velocities predicted by Eqs. (75) and (83). The geometric and loading parameters used are: (a, b):  $x_i = (0.2, 1.2, 1.4)$ ,  $\alpha_i = (0.1, 0., 0.1)$ ,  $\sigma_i = (1., 0., 0.1)$ . (c, d):  $x_i = (0.2, 1.2, 1.4)$ ,  $\alpha_i = (10., 0., 10.)$ ,  $\sigma_i = (1., 0., 0.1)$ . (e, f):  $x_i = (0.5, 1.5, 1.6)$ ,  $\alpha_i = (3., 0., 7.)$ ,  $\sigma_i = (0.98, 0., 0.23)$ . (g, h):  $x_i = (0.2, 1.2, 1.4)$ ,  $\alpha_i = (100., 0., 100.)$ ,  $\sigma_i = (1., 0., 0.)$ .

those shown in Fig. 3 were obtained. Details of the upwind procedure are described in Appendix D.

For a wide range of parameter values, we find very good agreement between the numerical and analytical solutions derived in the previous sections as shown in Fig. 3. In real plants, the size of the leaves is typically ~ 20% of that of the stem, and our choice of parameters in Figs. 3(a)–(d) and (g)–(h) reflects this. Other parameters are chosen with a large variation both to approach low and high values of the Münch number, and to validate and demonstrate the robustness of the solutions.

The solution for  $M\ddot{u} \ll 1$  accurately reproduces the numerical solutions for all parameter choices tested while, as expected, the solution for large  $M\ddot{u}$  is most accurate when the boundary layer thickness  $\lambda \sim (\alpha_3 M\ddot{u})^{-1}$  at  $x = x_2$  is very small compared to the unloading zone length  $x_3 - x_2$ . We note that the analytical solution for  $M\ddot{u} \ll 1$  is almost identical to the numerical solution for  $M\ddot{u} = 1$  and it even works well for  $M\ddot{u} = 10$ , particularly for the concentration  $c(x)$ .

### 5. Mean translocation velocity

As outlined in Section 2.1 and Fig. 1, the situation where the concentrations in the loading zone  $c_1$  and unloading zone  $c_3$  are close to the target values  $\sigma_1$  and  $\sigma_3 \ll \sigma_1$ , respectively, is of particular interest. This is illustrated in the examples in Figs. 3(g)–(h). From Eqs. (14) and (15), we see that this happens when  $\alpha_1, \alpha_3 \rightarrow \infty$ . Further assuming that the loading and unloading zones have equal lengths  $l_1 = l_3$ , we can compute the average translocation velocity  $\bar{u}$  in a very simple manner from the analytical solutions given in the previous sections.

#### 5.1. Mean translocation velocity $\bar{u}$ for $M\ddot{u} \ll 1$

In the translocation zone, the velocity is often approximately constant (see Fig. 3) and we may take the average value  $\bar{u}$  to be approximately equal to the velocity at the end of the translocation zone  $\bar{u} \simeq u_2(x_2)$ .

To compute  $u_2(x_2)$ , we use the results given in Table 1 with  $\sigma_3 \ll \sigma_1 \sim 1$ ,  $\alpha_1 \gg 1$ ,  $\alpha_3 \gg 1$ , and  $l_1 = l_3$  which yields

$$A_{1,1} = \frac{3 - \sqrt{5}}{2} \sigma_1, \tag{70}$$

$$A_3 = \frac{\sqrt{5} - 1}{2} \sigma_1, \tag{71}$$

$$A_4 = \frac{1 + \sqrt{5}}{2} l_1, \tag{72}$$

$$K_{1,3} = -\frac{\sqrt{5} - 1}{2} \sigma_1, \tag{73}$$

$$K_{2,1} = K_{2,3} = 0. \tag{74}$$

From Eq. (46), we then find that

$$\bar{u} \simeq u_2(x_2) = \frac{\sigma_1 A_{1,1} l_1}{A_3} = \frac{\sqrt{5} - 1}{2} l_1 \sigma_1 \simeq 0.62 l_1 \sigma_1. \tag{75}$$

As shown in Fig. 3(g), this expression gives a very good estimate of the velocity  $u_2(x_2)$ . Using the implicit loading scheme given in Eq. (10) with  $\sigma_1 = 1$ , Jensen et al. (2011) found a result similar to that given in Eq. (75)

$$\bar{u} = \frac{\sqrt{3} - 1}{2} l_1 = 0.37 l_1, \tag{76}$$

where the numerical difference in the prefactor between Eqs. (75) and (76) is most likely due to the difference in the loading mechanisms.

#### 5.1.1. Mean translocation velocity $\bar{u}$ for $M\ddot{u} \gg 1$

In general, the mean translocation velocity  $\bar{u}$  for large values of  $M\ddot{u}$  is given by

$$\bar{u} = \frac{1}{x_3 - x_2} \int_{x_2}^{x_3} u_2(x) dx = \frac{1 - \sqrt{1 - 2M\ddot{u} u_1(x_1) / c_1(x_1)}}{M\ddot{u}}. \tag{77}$$

To determine  $u_1(x_1)$ , we note that when evaluated at  $x = x_3$ , the expression for  $u_3$  in Eq. (66) is approximately

$$0 \simeq (B_4 + B_5) \exp(\sqrt{M\ddot{u}}(x_3 - x_2)), \tag{78}$$

such that

$$B_4 + B_5 = 0. \tag{79}$$

Assuming that  $c_1(x_1) \simeq \sigma_1$ , we can expand Eq. (79) to first order in  $u_1(x_1)$

$$\sqrt{M\ddot{u}}(\sigma_3 - \sigma_1) + \frac{(\alpha_3 + 2M\ddot{u}^{3/2} \alpha_3 + \sigma_1 - \sigma_3) u_1(x_1)}{\alpha_3} \simeq 0, \tag{80}$$

such that

$$u_1(x_1) \simeq \frac{\sqrt{M\ddot{u}}(\sigma_1 - \sigma_3) \alpha_3}{\alpha_3 + 2M\ddot{u}^{3/2} \alpha_3 + \sigma_1 - \sigma_3} \tag{81}$$

Applying the conditions  $\sigma_3 \ll \sigma_1 \sim 1$ ,  $\alpha_1 \gg 1$ , and  $\alpha_3 \gg 1$  we have that

$$u_1(x_1) \simeq \frac{\sigma_1}{2M\ddot{u}}. \tag{82}$$

From Eq. (77) we then find

$$\bar{u} \simeq \frac{1}{M\ddot{u}}, \tag{83}$$

the same as found by Jensen et al. (2011). As shown in Fig. 3(g), this expression gives a reasonable estimate of the mean velocity  $\bar{u}$ .

Combining Eqs. (75) and (83) yields an interpolation formula for  $\bar{u}$

$$\bar{u} = \frac{1}{\frac{m}{l_1 \sigma_1} + M\ddot{u}}, \tag{84}$$

where  $m = 2/(\sqrt{5} - 1)$ . In dimensional units, the velocity is

$$\bar{U} = 2 \frac{L_p R T C_{out} L}{r} \frac{1}{\frac{m}{l_1 \sigma_1} + M\ddot{u}}, \tag{85}$$

where we recall that  $l_1$  is the ratio of length of the loading zone, i.e., a typical leaf, to the length of the stem, and  $\sigma_1$  is the ratio of the target concentration of sugar in the loading zone to the concentration of sugar in the apoplast, i.e., of order 1. The interpolation formula in Eq. (85) is similar to results obtained using a simple resistor model (Jensen, 2011; Jensen et al., 2012).

### 6. Universal properties of the loading function

It is an interesting observation that most of the characteristic properties of the flow solutions discussed in Section 2.1 and illustrated in Fig. 1 are found in virtually all theoretical studies of Münch–Horwitz flow, across a broad range of loading functions  $\Upsilon$ , including that investigated here. This similarity has been noticed previously by several authors, e.g. Tyree et al. (1974) and more recently by Thompson and Holbrook (2003b), who noticed that their results were “qualitatively similar to the steady-state results of other workers” when referring to Christy and Ferrier (1973), Tyree et al. (1974), Goeschl et al. (1976).

Indeed we have observed that for a given loading function of the form  $\Upsilon = a + bc$ , an equivalent transformed concentration field  $\tilde{c}$  and loading function  $\tilde{\Upsilon} = \tilde{a}$  exists such that a solution of the

problem

$$\partial_x^2 u = \partial_x \tilde{c} + M\ddot{u}u, \quad (86)$$

$$\partial_x(\tilde{c}u) = \tilde{\gamma} = \tilde{a}, \quad (87)$$

also, at least approximately, solves the original problem for  $c$  with  $\gamma = a + bc$ . Here,  $\tilde{a}$  and  $\tilde{c}$  are functions of  $a$ ,  $b$ , and the boundary conditions of the flow problem.

We have not been able to prove this statement for arbitrary values of the Münch number  $M\ddot{u}$ , but we can give the following approximate argument. A characteristic feature of these flows is that the concentration  $c$  is approximately constant in the better part of the loading and unloading zones, see Fig. 1(b). This allows us to write the concentration  $c(x)$  as

$$c(x) \simeq c(0) = \frac{a}{\partial_x u(0) - b}, \quad (88)$$

where we have applied Eq. (14). We may thus approximate the (second) equation of motion as

$$\partial_x(cu) \simeq a + bc(0) = a + \frac{ab}{\partial_x u(0) - b}. \quad (89)$$

In this case, we find that a solution of the problem with

$$\tilde{\gamma} = \tilde{a} = a + \frac{ab}{\partial_x u(0) - b} = \frac{a}{1 - \frac{b}{\partial_x u(0)}} \quad (90)$$

also solves the general problem  $\gamma = a + bc$ .

### 6.1. Proof of the universality statement for $M\ddot{u} \ll 1$

In the limit of very small Münch numbers, we can prove the mathematical equivalence between the two types of loading functions directly. We begin by dropping terms of order  $M\ddot{u}$  in Eqs. (1)–(2), to find

$$\partial_x^2 u = \partial_x c, \quad (91)$$

$$\partial_x(cu) = a + bc. \quad (92)$$

Integrating the first equation yields

$$\partial_x u = c + k_1, \quad (93)$$

where  $k_1$  can be found from the boundary conditions at the end point  $x=0$ ,

$$k_1 = \partial_x u(0) - c(0) = \partial_x u(0) - \frac{a}{\partial_x u(0) - b} = \frac{\partial_x u(0)^2 - \partial_x u(0)b - a}{\partial_x u(0) - b}. \quad (94)$$

such that

$$\partial_x(cu) = a + b\partial_x u - bk_1. \quad (95)$$

We now realise that with  $\tilde{c} = c - b$  and  $\tilde{a} = a - bk_1$ , the equations of motion can be written as

$$\partial_x^2 u = \partial_x \tilde{c}, \quad (96)$$

$$\partial_x(\tilde{c}u) = \tilde{a}, \quad (97)$$

of the form given in Eqs. (86)–(87). Thus, for  $M\ddot{u} \ll 1$ , there is no difference between the concentration dependent and concentration independent loading functions.

## 7. Discussion

The modelling and confirmation of the Münch hypothesis for sap translocation in the phloem vascular system relies on specific sugar loading and unloading characteristics. We have shown that it is possible to obtain analytical solutions for the case of “target concentration” loading, where the concentration is guided towards an

external concentration set by the plant. We have presented analytical solutions for both very small and very large Münch numbers and, combined with numerical solutions, this gives us a rather complete understanding of the flow and its dependence on the external parameters such as concentrations, permeabilities and geometry. Motivated by similarity of flow structures and a direct equivalence for  $M\ddot{u} = 0$ , we further speculate that the basic properties of these flows are robust over a broad range of loading functions considered in the literature. We suggest therefore that future studies to understand, say, phloem flow in branched systems, may be based on the simplest possible mathematical choice of loading and unloading function.

Another interesting and biologically important result obtained is the mean flow velocity with an interpolation formula suggested in Eq. (84). It is reassuring that the results we obtain are readily comparable to results from a simple resistor-based hydraulic model (Jensen et al., 2012).

In conclusion, we believe that our analytic solutions for prototypic Münch–Horwitz equations will be useful to dispell some of the controversy surrounding the Münch hypothesis by providing accurate and easily accessible solutions for the fluid flows.

## Appendix A. Dimensional and dimensionless equations for osmotically driven flow

The basic equations, Eqs. (1)–(2), result from considering the flow in a circular pipe with a semi-permeable membrane cylindrical wall. We consider the dynamics along the axis of the cylinder, denoted  $X$  (carrying the physical dimension of a length). The membrane allows for both water and sugar to pass, with volume flux  $J_w$  and sugar molecule flux  $J_s$  given as

$$J_w = L_p(RT(C_{\text{out}} - C(X)) - (P_{\text{out}} - P(X))), \quad (A.1)$$

$$J_s = v, \quad (A.2)$$

where  $L_p$  is the hydraulic conductivity of the membrane (the permeability) and  $v$  is an as yet unspecified loading/unloading function. In the expressions for the flow rates,  $C_{\text{out}}$  is the (constant) sugar concentration outside the pipe and  $C(X)$  is that inside; similarly  $P_{\text{out}}$  is the constant outside pressure and  $P(X)$  the varying inside pressure. With the specific choice of a target-concentration loading/unloading function,  $J_s$  may be expressed as

$$J_s^{\text{target}} = -L_s RT(C_{\text{target}} - C(X)), \quad (A.3)$$

where  $L_s$  is the permeability for sugar.

Let  $U(X)$  denote the axial velocity of the water in the pipe. Then, conservation of volume in a small cross section of the pipe relates the velocity to concentration and pressure differences:

$$\partial_X U = \frac{2L_p}{r}(RT(C_{\text{out}} - C(X)) - (P_{\text{out}} - P(X))). \quad (A.4)$$

Here,  $r$  is the radius of the pipe.

In addition, conservation of the number of sugar molecules within a small section of the pipe implies

$$\partial_X(CU) = -\frac{2}{r}v, \quad (A.5)$$

which for the special case of a target-concentration loading/unloading function reads

$$\partial_X(CU)^{\text{target}} = -\frac{2L_s}{r}RT(C_{\text{target}} - C(X)). \quad (A.6)$$

In order to eliminate the pressure from the set of equations, we assume a low Reynolds number Poiseuille flow, i.e.,

$$U = -\frac{r^2}{8\eta}d_X P, \quad (A.7)$$

which can be combined with Eq. (A.4) differentiated once with respect to axial position, to find

$$\partial_x^2 U = \frac{2L_p RT}{r} \partial_x C + \frac{16L_p \eta}{r^3} U. \tag{A.8}$$

Eqs. (A.5) and (A.8) comprise our set of equations of motion.

We renormalise these equations by introducing the rescaling

$$X = Lx, \quad C(X) = C_{out}c(X), \quad U(X) = \frac{2L_p RTC_{out}L}{r} u(X), \tag{A.9}$$

where  $L$  is the length of the translocation zone in the loading-translocation-unloading system,  $C_{out}$  is the outside concentration of sugar in the loading zone, and  $r$  is the radius of the part of the plant corresponding to the translocation zone. If we insert these rescalings in our dimensional equations of motion, Eqs. (A.6) and (A.8), we obtain Eqs. (1)–(2) with the special loading/unloading function

$$\gamma_i = \alpha_i(\sigma_i - c(x)), \quad \alpha = \frac{L_s}{C_{out}L_p} \tag{A.10}$$

and the Münch number,  $M\ddot{u} = 16L_p \eta L^2 / r^3$  naturally appears. In Eq. (A.10),  $\sigma_i$  is the dimensionless ratio between the target concentration of zone  $i$  and the outside concentration  $C_{out}$  at the site of the loading zone.

**Appendix B. The constant concentration implicit loading scheme**

A very simple loading scheme is to assume that the concentrations in loading and unloading zones are both constant and that the flow direction is given by their relative strength. In this case we need not specify an explicit loading function and the governing equations are simply

$$\partial_x^2 u_1 = M\ddot{u}u_1(x), \quad 0 < x < x_1, \tag{B.1}$$

$$\partial_x^2 u_2 = \partial_x c_2 + M\ddot{u}u_2(x) = -\frac{u_1(x_1)c_1(x_1)}{u_2^2(x)} \partial_x u_2 + M\ddot{u}u_2(x), \quad x_1 < x < x_2, \tag{B.2}$$

$$\partial_x^2 u_3 = M\ddot{u}u_3(x), \quad x_2 < x < x_3, \tag{B.3}$$

where, as in Section 3.2.2, we use that  $c(x)u(x) = \text{constant}$ .

A meaningful solution  $u(x)$  of these equations with flow from the loading to the unloading zones must be nonnegative everywhere and approach zero in both ends. It must therefore have at least one maximum along the way. We now show that this is impossible. For this purpose, assume to the contrary that the translocation zone contains a maximum for  $u$ , say at  $x_m$ . Integrating Eq. (B.2) from a point  $x = x_a$  to a point  $x = x_b$  gives

$$u'(x_b) - u'(x_a) = c(x_b) - c(x_a) + M\ddot{u} \int_{x_a}^{x_b} u(x) dx \tag{B.4}$$

and, using  $u(x_a)c(x_a) = u(x_b)c(x_b)$ , this can be written

$$u'(x_b) - u'(x_a) = c(x_a) \left( \frac{u(x_a)}{u(x_b)} - 1 \right) + M\ddot{u} \int_{x_a}^{x_b} u(x) dx. \tag{B.5}$$

Having a maximum in  $u$  at  $x = x_m$  it is always possible to choose a position  $x_a < x_m$  and another position  $x_b > x_m$  so that  $u(x_a) = u(x_b)$ , and with  $u'(x_a) > 0$  and  $u'(x_b) < 0$  Eq. (B.5) reduces to

$$u'(x_b) - u'(x_a) = M\ddot{u} \int_{x_a}^{x_b} u(x) dx, \tag{B.6}$$

which is a contradiction, since the left hand side must be negative, and the right hand side must be nonnegative. This means that there can be no maximum in the velocity in the

translocation zone, and hence the velocity and its derivative must be positive throughout this zone.

In the source zone, the velocity  $u$  satisfies Eq. (B.1) and, with  $u(0) = 0$ , it has the solution

$$u(x) = A \sinh[\sqrt{M\ddot{u}}x] \tag{B.7}$$

with  $A > 0$  which obviously is monotonically increasing and can have no maximum. The sink zone is governed by the identical equation (B.3). The boundary conditions at the entry of this zone ( $x = x_2$ ) are given from the analysis above: both the velocity and its derivative are positive. The general solution is

$$u(x) = B_4 \exp[\sqrt{M\ddot{u}}(x-x_2)] + B_5 \exp[-\sqrt{M\ddot{u}}(x-x_2)]. \tag{B.8}$$

Applying the initial conditions gives two inequalities in the integration coefficients  $B_4$  and  $B_5$ ,

$$B_4 + B_5 > 0, \quad B_4 - B_5 > 0, \tag{B.9}$$

which readily implies that  $B_4 > 0$  and  $B_4 > |B_5|$ . With these coefficients both the velocity and its derivative are positive for all  $x > x_2$ , and hence, no maximum can exist in the sink.

We thus conclude that a maximum cannot exist. We have not explicitly considered the possibility of having a maximum exactly on the border between the translocation and unloading zone; however, it can be shown easily that the existence of such a maximum of  $u$  would prevent the velocity from becoming zero at  $x_3$ . Indeed, the solution which is zero at  $x = x_3$  must be of the form  $u(x) = A \sinh[\sqrt{M\ddot{u}}(x-x_3)]$  which is monotonic.

**Appendix C. Constant loading**

Our equations are

$$\partial_x^2 u = \partial_x c + M\ddot{u}u, \tag{C.1}$$

$$\partial_x(uc) = a. \tag{C.2}$$

Observe that in the constant loading model, conservation of the amount of sugar transported imposes restriction on the parameters. In other words, the amount of sugar loaded must equal the amount of sugar unloaded which implies that  $a_1x_1 = -a_3(x_3-x_2)$ . Solving Eq. (C.2) with  $u(0) = 0$  gives

$$uc = ax \tag{C.3}$$

and inserting this into the first equation gives the single equation

$$\partial_x^2 u + \frac{ax}{u^2} \partial_x u = M\ddot{u}u + \frac{a}{u}. \tag{C.4}$$

For large  $M\ddot{u}$ , we expect that  $u = V/M\ddot{u}$  where  $V$  is of order unity. Inserting this gives

$$\frac{1}{M\ddot{u}} \partial_x^2 u + \frac{M\ddot{u}ax}{V^2} \partial_x V = V + \frac{M\ddot{u}a}{V}. \tag{C.5}$$

If we now assume that  $a$  becomes very small in this limit, i.e.  $a = A/M\ddot{u}$ , where  $A$  is of order unity, we get

$$x \partial_x V = \frac{V^3}{A} + V, \tag{C.6}$$

where we have neglected the term  $\partial_x^2 u$  of order  $1/M\ddot{u}$ . Note that it is the term of highest order. Introducing  $t = \ln x$  Eq. (C.6) can be written as

$$\frac{dt}{dV} = \left( \frac{V^3}{A} + V \right)^{-1} \tag{C.7}$$

with the solution

$$t = A \int^V \frac{dz}{z^2(z+A)} = \int^V dz \left( \frac{1}{z^2} + \frac{1}{A(z+A)} - \frac{1}{Az} \right) \tag{C.8}$$

**Table E2**

The parameters used in the paper are listed in alphabetical order in Table E2. All parameters are non-dimensional unless otherwise stated.

Parameter	Symbol/expression
Integration constants:	
in loading zone	$A_1, B_1, B_2, K_{2,1}, k_1, D$
in translocation zone	$A_3, A_4$
in unloading zone	$B_3, B_4, B_5, K_{1,3}, K_{2,3}, K_{3,3}, k_1$
Loading rate	$a$
in zone $i$	$a_i$
Loading parameter	$b$
in zone $i$	$b_i$
Concentration	$c$
in zone $i$	$c_i$
Concentration in dimensional units	$C$ (mol/m <sup>3</sup> )
in the apoplast	$C_{out}$ (mol/m <sup>3</sup> )
target value	$C_{target}$ (mol/m <sup>3</sup> )
Zone number	$i=1,2,3$
Volume flux of water	$J_w$ (m <sup>3</sup> /(m <sup>2</sup> s))
Molecule flux of sugar	$J_s$ (mol/(m <sup>2</sup> s))
Plant length, physical length of translocation zone	$L$ (m)
Membrane permeability	$L_p$ (m/(Pa s))
Membrane permeability for sugar	$L_s$ (mol/(m <sup>2</sup> Pa s))
Length of zone $i$	$l_i$
loading zone	$l_1 = x_1$
translocation zone	$l_2 = x_2 - x_1 = 1$
translocation zone	$l_3 = x_3 - x_2$
Münch number	$M\ddot{u}$
Geometric parameter	$m = \frac{2}{\sqrt{5}-1}$
Pressure	$p$
Pressure in dimensional units	$P$ (Pa)
outside the phloem tube	$P_{out}$ (Pa)
Sieve tube radius	$r$ (m)
Flow velocity	$u$
in zone $i$	$u_i$
Flow velocity in dimensional units	$U$ (m/s)
Average flow velocity	$\bar{u}$
Scaled flow velocity	$v = u/x$
Flow velocity (in Appendix C)	$V = uM\ddot{u}$
Axial coordinate	$x$
Zone start/end points	$x_i$
Axial coordinate	$z = \log x$
Loading rate	$\alpha$
in zone $i$	$\alpha_i$
Concentration gradient	$\beta$
Partial differentiation with respect to $x$	$\partial_x$
Relative concentration	$\epsilon = \sigma - c$
Boundary layer thickness	$\lambda$
Viscosity	$\eta$ (Pa s)
Loading function	$\Upsilon$
in zone $i$	$\Upsilon_i$
Loading function in dimensional units	$v$ (mol/(m <sup>2</sup> s))
Target concentration	$\sigma$
in zone $i$	$\sigma_i$

$$= -\frac{1}{V} + \frac{1}{A} \ln\left(\frac{V+A}{V}\right) + \text{const} \quad (\text{C.9})$$

or

$$x = De^{-1/V} \left(\frac{V+A}{V}\right)^{1/A} \quad (\text{C.10})$$

## Appendix D. Numerical solution methods

When solving the equations of motion (Eqs. (1)–(2)) by reducing the equation system to three first order differential equations and solving these using standard techniques, one often encounter difficulties near  $x=0$  where the velocity is very small.

To avoid these problems, we used the upwind method (Press, 2001). Dividing each zone of length  $\ell$  into a set of discrete points  $x_n$ ,  $n=1, \dots, N$  we write for  $\partial_x u$ ,  $\partial_x^2 u$ , and  $\partial_x c$  that

$$\partial_x u(x_i) \approx \frac{u(x_i) - u(x_{i-1}))}{\Delta x}, \quad (\text{D.1})$$

$$\partial_x^2 u(x_i) \approx \frac{u(x_i) - 2u(x_{i-1}) + u(x_{i-2}))}{\Delta x^2}, \quad (\text{D.2})$$

$$\partial_x c(x_i) \approx \frac{c(x_i) - c(x_{i-1}))}{\Delta x}, \quad (\text{D.3})$$

where  $\Delta x = \ell/N$ , and  $N$  was chosen such that  $\Delta x$  were of the order  $10^{-5}$ . The name upwind comes from the fact that differentials of, say, the velocity  $u$ , is approximated by  $u(x_i) - u(x_{i-1})$  and not  $u(x_{i+1}) - u(x_i)$  or  $u(x_{i+1}) - u(x_{i-1})$ .

From Eqs. (D.1)–(D.3), the solution of the equations of motion were approximated numerically in each of the zones by

$$u(x_i) \approx \frac{1}{1 - \Delta x^2 M\ddot{u}} [2u(x_{i-1}) - u(x_{i-2}) + \Delta x(c(x_{i-1}) - c(x_{i-2}))], \quad (\text{D.4})$$

$$c(x_i) \approx \frac{1}{2u(x_i) - u(x_{i-1}) + \Delta x \alpha} [u(x_i)c(x_{i-1}) + \Delta x \alpha \sigma]. \quad (\text{D.5})$$

Starting at  $x=0$ , the solver ran with the flow, i.e. from zone  $1 \rightarrow 2 \rightarrow 3$ , ensuring that all internal boundary conditions were fulfilled. Finally, the boundary condition at  $x=x_3$  was fulfilled by varying  $\partial_x u$  at  $x=0$  until  $u(x_3)$  was less than a tolerance  $\tau$ , chosen to be of the order  $10^{-10}$ .

## Appendix E. List of parameters

The parameters in alphabetic order after the symbol are listed in Table E2. All parameters are non-dimensional unless otherwise stated.

## References

- Christy, A.L., Ferrier, J.M., 1973. Plant Physiol. 52, 531–538.
- Eschrich, W., Evert, R.F., Young, J.H., 1972. Planta (Berl.) 107, 279–300.
- Goeschl, J.D., Magnuson, C.E., 1986. Plant, Cell & Environ. 9, 95–102.
- Goeschl, J.D., Magnuson, C.E., Demichele, D.W., Sharpe, P.J.H., 1976. Plant Physiol. 58, 556–562.
- Horwitz, L., 1958. Plant Physiol. 33, 81–93.
- Jensen, K.H., 2011. Osmotically Driven Flows in Microfluidic Systems and Their Relation to Sugar Transport in Plants. Ph.D. Thesis, Department of Micro- and Nanotechnology, Technical University of Denmark.
- Jensen, K.H., Rio, E., Hansen, R., Clanet, C., Bohr, T., 2009a. J. Fluid Mech. 636, 371–396.
- Jensen, K.H., Lee, J., Bohr, T., Bruus, H., 2009b. Lab on a Chip 9, 2093–2099.
- Jensen, K.H., Lee, J., Bohr, T., Bruus, H., Holbrook, N.M., Zwieniecki, M.A., 2011. J. R. Soc. Interface 8, 1155–1165.
- Jensen, K.H., Liesche, J., Bohr, T., Schulz, A., 2012. Plant Cell Environment. Knoblauch, M., Peters, W.S., 2010. Plant Cell Environment 33, 1439–1452.
- Lacointe, A., Minchin, P.E.H., 2008. Functional Plant Biology 35, 772–780.
- Magnuson, C.E., Goeschl, J.D., Fares, Y., 1986. Plant, Cell & Environment 9, 103–109.
- Maynard, J.W., Lucas, W.J., 1982. Plant Physiol. 69, 734–739.
- Minchin, P.E.H., Thorpe, M.R., Farrar, J.F., 1993. J. Exp. Bot. 44, 947–955.
- Münch, E., 1930. Die Stoffbewegung in der Pflanze. Jena, Verlag von Gustav Fisher.
- Phillips, R.J., Dungan, S.R., 1993. J. Theor. Biol. 162, 465–485.
- Pickard, W.F., Abraham-Shrauner, B., 2009. Funct. Plant Biol. 36, 629–644.
- Press, W.H., 2001. Numerical Recipes in Fortran 77, vol. 1, second ed. Cambridge University Press.
- Smith, K.C., Magnuson, C.E., Goeschl, J.D., DeMichele, D.W., 1980. J. Theor. Biol. 86, 493–505.
- Thompson, M.V., Holbrook, N.M., 2003a. Plant, Cell Environ. 26, 1561–1577.
- Thompson, M.V., Holbrook, N.M., 2003b. J. Theor. Biol. 220, 419–455.
- Thompson, M.V., Holbrook, N.M., 2003c. Plant, Cell Environ. 26, 1561–1577.
- Thompson, M.V., Holbrook, N.M., 2004. Plant, Cell Environ. 27, 509–519.
- Thompson, M.V., 2005. J. Theor. Biol. 236, 229–241.
- Thompson, M.V., 2006. Trends Plant Sci. 11, 26–32.
- Turgeon, R., 1989. Annu. Rev. Plant Physiol. Plant Mol. Biol. 40, 119–138.
- Tyree, M.T., Christy, A.L., Ferrier, J.M., 1974. Plant Physiol. 54, 589–600.